Effect of solar insolation on a solar kiln performance

Khamtan Phonetip[1,*], Graham Ian Brodie[2] and Hilary Smith[3]

Faculty of Forest Science, National University of Laos, Vientiane Capital, Lao PDR

[1*]Correspondence:

Khamtan PHONETIP

Faculty of Forest Science, National University of Laos, Lao PDR,
Tel: +856 20 22206926
Email: khamtanfof@gmail.com

[2] Faculty of Veterinary and Agricultural Sciences, The University of Melbourne, Dookie Campus, Nalinga Rd., Dookie, Victoria 3647 Australia

[3] Fender School of Environment and Society, Australian National University, Canberra 2601, Australia

Article Info:
Submitted: Feb 11, 2022
Revised: Mar 17, 2022
Accepted: Mar 27, 2022

Abstract

This research aimed to investigate the effect of solar insolation on the internal temperature of a solar kiln at different levels of relative humidity (RH=20%, RH=40% & RH=60%), and create mathematical modelling to simulate the solar kiln conditions. A solar kiln was installed at the National University of Laos, Faculty of Forest Science under the Department of Forest Economics and Wood Technology in June 2021, this apparatus was used in this study. The recharge and discharge model was used to predict the solar kiln temperature. The results showed that solar insolation is an important contributor to a solar kiln's performance; however, it is not the only contributor. The solar kiln's temperature follows a thermal recharge phase during the morning and a thermal discharge phase during the afternoon and nighttime. The set value of relative humidity and present value of relative humidity inside the solar kiln also strongly influence the solar kiln temperature. The solar kiln can provide a free source of heat up to 54ºC, this could contribute to the wood processing sector in reducing the GHG emissions through drying timber using solar kiln method, with continuous drying technique or the combination with traditional kiln which would reduce the 60% of carbon emission from a drying batch.

Keywords: *Solar drying, Solar radiation, Solar kiln performance, drying timber.*

1. Introduction

Globally, the issue of greenhouse gas (GHG) emissions has been widely discussed and a range of international and national responses have been instigated In the Lao People's Democratic Republic (Laos) for instance, the government ratified the United National Framework Convention on Climate Change (UNFCCC) and the Kyoto Protocol in 2003. It has developed a climate change strategy, which builds on the country's commitment to its climate change adaption efforts (UNDP, 2012) and has prioritised green and sustainable development in its vision to 2030 of strategy on Socio-Economic Development Plan to 2025 (Ministry of Planning and Investment, 2016) and National Green Growth Strategy (GOL, 2018). The contribution of the wood processing sector to GHG emissions occurs through a range of direct and indirect activities (FAO 2010), including directly through the use of electricity and fossil fuels in equipment operations. In Laos emissions are also produced during wood drying because most kilns are steam kilns which use wood off cuts as fuel (Redman, 2016), and while these emissions are generally considered to be preferable, they can still be significant. Using wood fuel for energy can produce up to 60% carbon emission of a drying batch (Wibe, 2012). Using solar

kilns to dry wood is an alternative method that can reduce dependency on wood for fuel there by reducing emissions, and it is potentially economically beneficial because drying timber using a solar kiln can faster than the alternative low-emissions option - air drying (Armstrong & Hall, 1914), and when used in combination with a steam kiln can reduce costs (Phonetip et al., 2017).

There are various designs for solar kilns that have been used in the timber industry and for food drying for decades, including, for example, indirect and direct heat, and others (Sattar, 1993). However, choosing the right kiln design based on product requirements and situational conditions is needed to maximize productivity. Requirements may include affordability in construction, particularly in developing countries, and the structural design to enable optimal drying productivity. Further, because geographical conditions can affect drying time (Hasan & Langrish, 2014), consideration of location specific conditions is essential.

Vientiane, the capital city of Laos, is located in the tropics in an area with high solar radiation; conditions which are considered to be the most suitable for solar kiln technology (Simpson & Tschernitz, 1989). According to climatic data for Vientiane, the temperatures reach 40^{o}C in summer (December until April) with the lowest relative humidity (RH) in the range of 30-40% (S. NASA, 2014). Initial testing using a conventional laboratory kiln to simulate solar cyclic drying found that using the lowest level of RH of 40% and by replicating the conditions in Vientiane, wood can dry 50% faster than when the RH is 60% (Phonetip et al., 2017). However, confirmation based on experimental results required from the solar kiln is needed to understand the effects of solar insolation on the solar kiln performance.

A GIS-based fuzzy method was subsequently developed to identify suitable locations and optimal calendar months for running a solar kiln in Vientiane (Phonetip et al., 2018), and the research also identified the need for site visits to confirm site suitability prior to installation. Following site identification, a solar kiln was built at the National University of Laos (Phonetip et al., 2021).

This study investigated the effect of solar insolation on the internal temperature of a solar kiln at different levels of relative humidity, and create mathematical modelling to simulate the solar kiln conditions.

2. Materials and Methods

2.1 Equipment

A solar kiln was installed at the National University of Laos, Faculty of Forest Science under the Department of Forest Economics and Wood Technology in June 2021 (Phonetip et al., 2021) with the support of the Australian Center for International Agriculture Research (ACIAR).

The solar kiln's was constructed with a drying compartment, where the wood samples can be placed for drying and monitoring, with dimension of 1m x 1m x 2m, as shown in Figure 1. A heat controller was built using polyethylene foam coated with zinc, with the outer parts painted black. A transparent plastic sheet 0.15 μm thick was attached using spring wire clips at the edges. The kiln controller has two parts: the solar power source and kiln controller units. The solar power unit consists of a 200W solar panel, a solar charger with 30A, DC to AC converter (3000W) and a battery of 95Ah (FB Battery, M-1700 (105D31-MF)). The kiln controller unit consists of Aduino UNO boards with embedded codes to control two fans that extract heat from the heat collector, a circulating fan that is installed inside the kiln's compartment, and a water pump for controlling the relative humidity inside the kiln compartment Laos (Phonetip et al., 2021).

Using temperature and humidity sensors, the Aduino UNO uses an SD card module to monitor and store the temperature and relative humidity inside the kiln's compartment and heat collector. The data acquisition unit is controlled by an Arduino Uno with a DHT22 (temperature

and relative humidity) sensor. The accuracy of the DHT22 sensor, for humidity is ±2 %RH (Max ± 5%RH) and for temperature is <±0.5 Celsius (Liu, 2021). The temperature and relative humidity are recorded every 6 minutes and stored on the SD card. The RH was set and controlled by a water pump, based on the setting value read by DHT22 for RH. The water pump is "off" when the RH was higher than the set value and "on" when the RH was lower than the set value. The temperature was also set and controlled by two inlet fans through a heating induction pipe from the heat collector. The fans are "on" until the set temperature is reached and "off" when the temperature is higher or at the set value. The sketch coding was embedded in the Arduino Uno board using Arduino Integrated Development Environment (IDE) software (Open source).

2.2 Experiment

Experiments were conducted with three repetitions based on three different levels of RH set for the kiln conditions. A kiln temperature model used for predicting temperature inside a solar kiln was derived from Brodie (2005) and Phonetip et al., (2019a). This suggested that the maximum temperature inside a kiln over a 24-hour period was 55°C. The oscillation of temperature is plotted in Figure 2. Thus, in this study, the temperature was set at 60°C. The solar kiln operated from 8 AM until 5 PM. This was repeated for 10 days for each experiment without timber inside the solar kiln. The conditions of the three experiments are shown in Table 1.

2.4 Assessment method

A linear correlation was used to check the relationship between the solar insolation during the experiments in April, May and June of 2021, based on the data obtained from (P. NASA, 2021) at the geographical location of the kiln (Latitude of 18.041 and Longitude of 102.631). The conditions of the solar kiln's performance that was recorded by using the Arduino-SD card shield module (Phonetip et al., 2021). A mathematical model, created using Matlab software version R2021a (Mathworks, 2021), was used to determine the expected solar insolation at the kiln's location.

2.3 Modelling the drying dynamics

Modelling the temperature inside a solar drying kiln is a two-part consideration. Firstly, it is necessary to model the daily insolation (i.e., the amount of solar energy falling on the Earth). Secondly, it is necessary to determine how this insolation affects temperatures inside a solar kiln.

The daily fluctuations in solar activity depend on the angular velocity of the Earth, which is given by:

$$W = \frac{2\pi}{(24\times60\times60)} \quad (1)$$

It is also necessary to consider the geographic location of the kiln. Mathematically, the latitude needs to be expressed in Radians:

$$K_l = -\frac{Lat\cdot\pi}{180} \quad (2)$$

Where W is angular velocity of the Earth (radians s-1); K_l is location of solar kiln based on latitude (radians); Lat is latitude value obtained from the installed solar kiln.

Solar energy reaching the Earth depends on the distance of the earth from the sun (r), which is given by:

$$\frac{1}{r^2} = (1.000110 + 0.034221\cos\theta - 0.001280\sin\theta - 0.000719\cos 2\theta - 0.000077\sin 2\theta) \quad (3)$$

Solar declination (Ψ), which is the latitude of the sun's position on the Earth's surface, can be calculated using:

$$\psi = 0.006918 - 0.399912\cos\theta + 0.070257\sin\theta - 0.006758\cos 2\theta + 0.000907\sin 2\theta - 0.002697\cos 3\theta + 0.00148\sin 3\theta \quad (4)$$

These equations depend on the location of the Earth in its annual orbit; therefore, the orbit angle of the earth on the n^{th} day of the year is calculated using:

$$\theta = \frac{2\pi(n-1)}{365} \qquad (5)$$

Where θ the orbit angle and n is is the day number in the current solar year.

From an Earth-bound observer's perspective, the Sun follows an arc across the sky, where the altitude of the Sun above the horizon influences the intensity of the incoming solar radiation on a horizontal surface on the ground. The Sine of the solar altitude angle in the sky (SinAlt) can be calculated used:

$$SinAlt = \{sin(K_l) \cdot sin(\psi) + cos(K_l) \cdot cos(\psi) \cdot cos[600 \cdot W(t_2 + 600)]\} \qquad (6)$$

Where t_2 is the time of interest during the thermal charging period during the morning.

There is some attenuation of the incoming solar radiation as it passes through the atmosphere, even when there is no cloud cover. Atmospheric attenuation accounts for approximately 30 % of the incoming solar radiation; therefore, the atmospheric transmission coefficient (At) = 0.7.

The solar power falling onto the ground (P_s) can then be determined using:

$$P_s = \frac{1353 \cdot A_t \cdot SinAlt}{r} \qquad (7)$$

The solar kiln will undergo a thermal recharge phase during the morning and a thermal discharge phase during the afternoon and nighttime. The thermal recharge temperature (t_k) is described by:

$$t_k = a \times P_s + t_m \qquad (8)$$

The thermal discharge temperature (t_c) can be described by:

$$t_c = (E_t - S_t)e^{-C_r(t_1+300)} \qquad (9)$$

where E_t is end-temperature; S_t is start-temperature; C_r is Cooling Rate (determined experimentally for each kiln); a is Kiln Coefficient (also determined experimentally for each kiln); t_m is minimum ambient temperature; and t_1 is the time during the afternoon, after solar maximum, as the thermal energy from the solar kiln discharges. The time during the afternoon (t_1) is calculated as the difference between local time at the location of the kiln, after thermal maximum has been reached inside the kiln, and the time at which this thermal maximum occurs. The cooling rate C_r was based on a first-order discharge function that allowed energy discharge in the time between thermal maximum and thermal minimum. The cooling rate (C_r) is the slope of the natural logarithm of kiln temperature (i.e., ln(t_c)) as a function of time from thermal maximum and thermal minimum.

3. Results

Three important factors were identified i) solar kiln temperature can be affected by the level of RH inside the solar kiln, ii) understanding the effects of solar radiation on the solar kiln temperature is necessary to forecast the internal temperature, and iii) solar insolation has a significant effect on internal temperature this declines with increasing internal RH.

3.1 Solar kiln temperature can be affected by RH inside the kiln

The first of these is related to the set value for RH and solar insolation. The oscillation of the temperature inside the solar kiln (SK_t) is shown in Figure (2a) and the RH is shown in Figure (2b). The maximum temperature in the kiln reached an average temperature of 54°C±1 at 13.30 PM when the set value was 60°C and set value of the relative humidity (RH_{sv}) was 20%. Similarly, when the set temperature was 60°C, the maximum temperatures were 45°C±2, with RH_{sv} = 40%RH and 40°C±3 when RH_{sv} =60%RH. The maximum temperature dropped by 5°C when the RH_{sv} was changed from 20%

to 40% and it dropped by another 5°C when the set RH_{sv} was changed from 40% to 60%.

Figure 3 shows the linear relationship between the minimum RH_{pv} and RH_{sv}. There is a high correlation (R^2=0.99) between the set relative humidity RH_{sv} and the minimum RH_{pv}. Therefore, based on this study, this relationship can be used by an operator to properly set the solar kiln, i.e. if 30% RH of solar kiln is required then set value should be set at 20%RH using the function: RH_{pv} = 0.7153 RH_{sv} + 17.254.

3.2 Solar radiation affects internal temperature

Understanding the effects of solar radiation on the solar kiln temperature is necessary to forecast the temperature that could be reached inside the solar kiln. Figure 4 shows the oscillation of the insolation as a function of time from 8.00AM until 5.00PM. The insolation begins from 500 W/m^2 and rises to the maximum of 1000 W/m^2 at 12.00PM (P. NASA, 2021). This level of the insolation is similar to the levels of insolation at Melbourne, Australia (37°49'46.2"S 145°01'25.7"E) (Phonetip, Brodie, et al., 2019a). Figure 4 also shows the temperatures recorded in the solar kiln for different RH settings. While the temperature inside the kiln rises consistently with the insolation during the morning recharge period, it does not follow the insolation after 12:00PM. This is in accordance with the thermal recharge phase during the morning and a thermal discharge phase during the afternoon

3.3 Solar insolation affects internal temperature

While solar insolation has a significant effect on temperature inside the solar kiln, as shown in

Figure 5, the solar kiln temperature declines with increasing RH inside the solar kiln

Figure 5, (a), (b) and (c). For example, the temperature inside the solar kiln at the RH_{sv} = 20% is higher than when RH_{sv} is set for 40% and 60% with R^2=0.92, R^2=0.94, R^2=0.96, respectively. This means that operating the solar kiln must allow for the fact that higher RH inside the solar kiln will decrease the internal temperature during its operational period from April to June in Vientiane, Lao P.D.R.

Therefore, the set value of RH, the present value of RH inside the solar kiln and the solar insolation all affect the solar kiln temperature. Solar kiln temperature (SK_t) as a function of RH_{sv}, RH_{pv} and solar insolation can be expressed as

$$SK_t = 60.8689 + RH_{sv} \times 0.02920 + RH_{pv} \times (-0.4198) + Insolation \times 0.0023 \quad (10)$$

The goodness of fit for this relationship is R^2= 0.97.

A simple way to visualize the performance of a mathematical model is to plot the measured parameter against the predictions of the model. A line, with a slope approaching 1.0, should fit through the resulting plot. Figure 6 shows this plot, demonstrating the predictive power of equation (10).

Figure 6 shows the predictive power of equation (8 & 9) for the measured solar kiln temperature and the predicted solar kiln temperature. The R2=0.9 for RH = 20 %, 0.88 for RH = 40 % and 0.89 for RH = 60 %. These figures help to check the relation of each set value of the RH.

4. Discussion

The maximum of temperature for the set value of 20% was higher than the application used for drying a standing teak tree by 18°C in average even though the area of heat collector was the same (9m^2) (Phonetip et al., 2021). This means that the material that was used for the heat controller in this solar kiln, which was built using 5mm thick polyethylene foam coated with zinc, can generate a higher temperature than the black plastic sheet that was used in the previous study in Vientiane, Laos (Phonetip et al., 2021). Therefore, if this polyethylene foam coated with zinc is used in other geographical locations, like in Australia, it might also result in higher temperatures inside solar kilns (Phonetip, et al.,

2019b; Ozarska, et al., 2019). As of the results of providing RH at different levels can affect the temperature inside the solar kiln, this could imply as of an addition of the effects on the drying time based on the geographical conditions (Hasan & Langrish, 2014). Moreover, there are various designs for solar kilns that have been used in the timber industry with different efficiency (Sattar, 1993).

When RH_{sv} is set to 20% the RH_{pv} reaches a minimum of 30%±7 at 14.00 PM, RH_{sv} (40%) results in a minimum RH_{pv} of 45%±3, which is maintained from 11.30 AM until 15.00 PM, and RH_{sv}(60%) results in a minimum RH_{pv} of 60%±11 from 12.00 until 15.00. Therefore, the RH_{pv} increases by approximately 15 % intervals as RH_{sv} lifted from 20% to 40% and from 40% to 60%. The maximum of the RH_{pv} is 10% above the RH_{sv} of 20%, 5% for RH_{sv} of 40%, and 0% RH_{sv} of 60%. The RH inside the solar kiln ranged from 26%-30% when the RH_{sv} was 20%, which was below the ambient conditions (35%) that were found near (20m) the current experimental site (Phonetip et al., 2021). In this experiment, cool water (at ambient conditions) was used to provide RH inside the solar kiln, thus, this might be the main effects on the temperature level inside the solar kiln as of the results in the figure 7.

5. Conclusion

Solar insolation is an important contributor to a solar kiln's performance; however, it is not the only contributor. The solar kiln's temperature follows a thermal recharge phase during the morning and a thermal discharge phase during the afternoon and nighttime. The set value of relative humidity and present value of relative humidity inside the solar kiln also strongly influence the solar kiln temperature.

Since the solar kiln can provide a free source of heat up to 54ºC, this could contribute to the wood processing sector in reducing the GHG emissions through drying timber using solar kiln method, with continuous drying technique or the combination with traditional kiln which would reduce the 60% of carbon emission from a drying batch. In addition, a further experiment should be undertaken to investigate the effect of using available warm water to generate the relative humidity inside the solar kiln. It is believed that if providing available warm water instead of cool water for the relative humidity at high level would increase the temperature inside the solar kiln as it occurred the figure 7(a).

6. Conflict of Interest

We certify that there is no conflict of interest with any financial organization regarding the material discussed in the manuscript.

7. Acknowledgments

Authors would like to thank VALTIP3-ACIAR (Project No. FST/2016/151) for providing fund of this publication.

8. References

Armstrong, J., & Hall, C. (1914). Wood Industry Factsheet (DR-1; Solar Drying Basics). West Virginia University. https://www.woodweb.com/knowledge_base_images/zp/solar_drying_ basics.pdf

Brodie, G. (2005). Microwave timber heating and its application to solar drying.

Food and Agriculture Organization of The United Nations. (2000). Impact of the global forest industry on atmospheric greenhouse gases. FAO Forestry Paper, 159.

Government Office. (2018). National Green Growth Strategy of the Lao P.D.R till 2030.

Hasan, M., & Langrish, T. A. G. (2014). Numerical Simulation of a Solar Kiln Design for Drying Timber with Different Geographical and Climatic Conditions in Australia. Drying Technology, 32(13), 1632–1639. https://doi.org/10.1080/07373937.2014.915556

Liu, T. (2021). Digital-output relative humidity & temperature sensor/module DHT22.

https://www.sparkfun.com/datasheets/Sensors/Temperature/DHT22.pdf

Mathworks. (2021). Matlab R2021a. Mathworks, Inc. https://www.mathworks.com/?s_tid=gn_logo

Ministry of planning and investment. (2016). Vision to 2030 of strategy on scio-economic development plant to 2025. https://rtm.org.la/wp-content/uploads/2017/08/Vision2030-and-10-Year-SocioEconomic-Dev-Strategy-2016_2025-LAO.pdf

NASA, P. (2021). Prediction Of Worldwide Energy Resource. https://power.larc.nasa.gov/data-access-viewer/

NASA, S. (2014). NASA Surface meteorology and Solar Energy Tables. https://eosweb.larc.nasa.gov

Phonetip, k., Boupha, L., Phanouvong, B., Sichaluene, O., Khammanivong, K., & Bouaphavong, D. (2021). Drying a Standing Teak Tree using a Solar Kiln Drying Method. Walailak Journal of Science and Technology (WJST), 18(8), Article 9384 (7 pages). https://doi.org/10.48048/wjst.2021.9384

Phonetip, K., Brodie, G. I., Ozarska, B., & Belleville, B. (2019a). Drying timber in a solar kiln using an intermittent drying schedule of conventional laboratory kiln. Drying Technology, 37(10), 1300–1312. https://doi.org/10.1080/07373937.2018.1496337

Phonetip, K., Brodie, G. I., Ozarska, B., & Belleville, B. (2019b). Drying timber in a solar kiln using an intermittent drying schedule of conventional laboratory kiln. Drying Technology, 37(10), 1300-1312. https://doi.org/10.1080/07373937.2018.1496337

Phonetip, K., Latsamy Boupha, Sithatha Boupha, & Somxay Khamboudaphanh. (2021). Designing and building a solar kiln suitable for Vientiane's geography and climate, Laos [Technical report]. VALTIP3. laoplantation.org

Phonetip, K., Ozarska, B., Belleville, B., & Brodie, G. I. (2017). Using a conventional laboratory kiln as a simulation of a solar cyclic drying. Division 5 Conference. IUFRO, Vancouver, Canada.

Phonetip, K., Ozarska, B., Brodie, G. I., Belleville, B., & Boupha, L. (2018). Applying a GIS-based Fuzzy Method to Identify Suitable Locations for Solar Kilns. BioResources; Vol 13, No 2 (2018). https://ojs.cnr.ncsu.edu/index.php/BioRes/article/view/Biores_13_2_2785_Phonetip_GIS_Fuzzy_Method_Solar_Kilns

Phonetip, K., Ozarska, B., Harris, G., Belleville, B., & Brodie, G. I. (2019). Quality assessment of the drying process for Eucalyptus delegatensis timber using greenhouse solar drying technology. European Journal of Wood and Wood Products, 77(1), 57–62. https://doi.org/10.1007/s00107-018-1364-2

Redman, A. (2016). Drying operations and dried quality study, and recommendations for improved drying efficiency. laoplantation.org

Sattar, M. A. (1993). Solar drying of timbe-A review. Holz Als Roh- Und Werkstoff, 51(6), 409-416. https://doi.org/10.1007/BF02628239

Simpson, W., & Tschernitz, J. (1989). Performance of a solar/wood energy kiln in tropical latitudes. Forest Product Journal, 39(1).

UNDP, L. (2012). National Strategy on Climate Change of Lao PDR. http://www.la.undp.org/content/lao_pdr/en/home/library/environment_energy/climate_change_strategy.html.

Wibe, S. (2012). Carbon dioxide emissions from wood fuels in Sweden 1980–2100. Journal of Forest Economics, 18(2), 123–130. https://doi.org/10.1016/j.jfe.2011.11.003

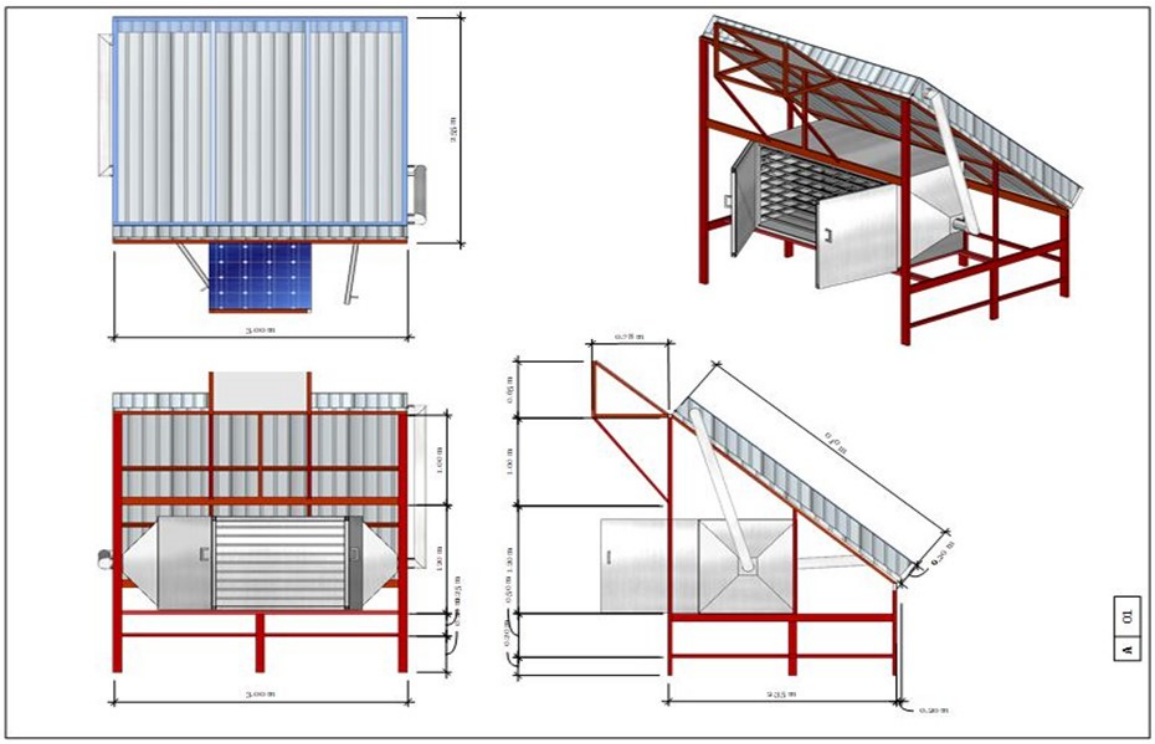

Figure 1. A solar kiln at the Faculty of Forest Science, National University of Laos

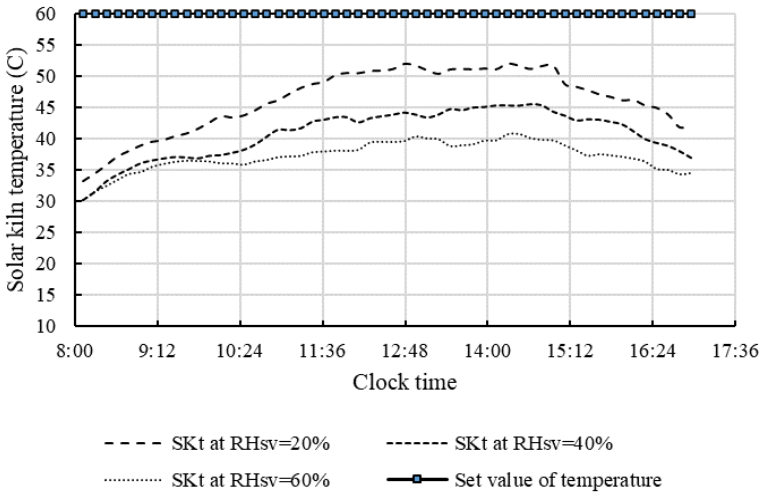

Figure 2a. The oscillation of temperature inside a solar kiln at set values for RH of 20%, 40% and 60%

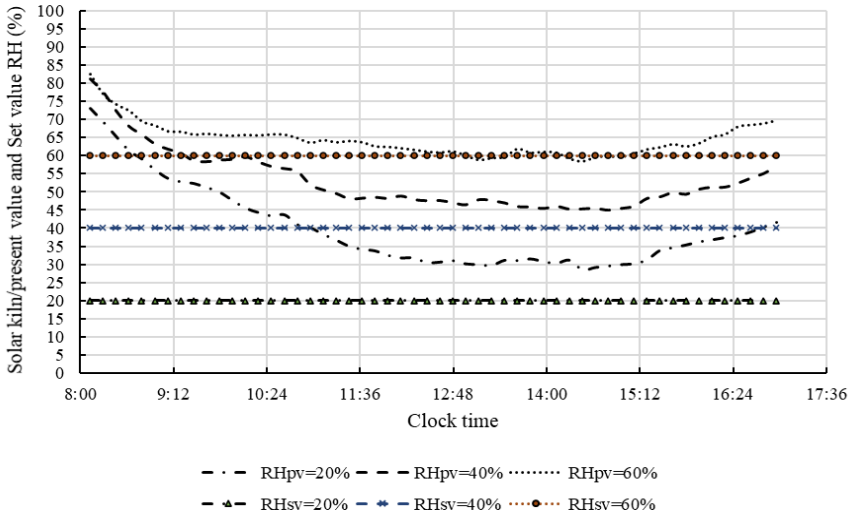

Figure 2b. The relative humidity inside a solar kiln at set values for RH of 20%, 40% and 60%

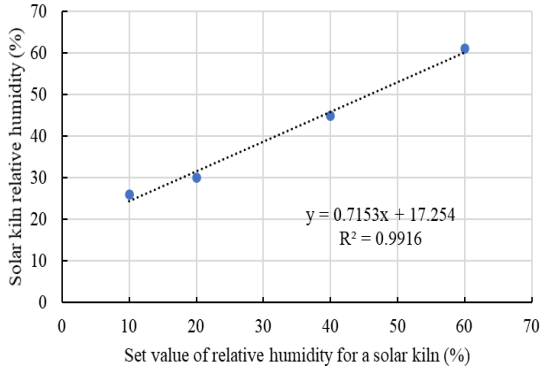

Figure 3. Correlation between set value of relative humidity (RHsv) and solar kiln relative humidity (RHpv) and nighttime, outlined in the theoretical study of solar kilns presented earlier.

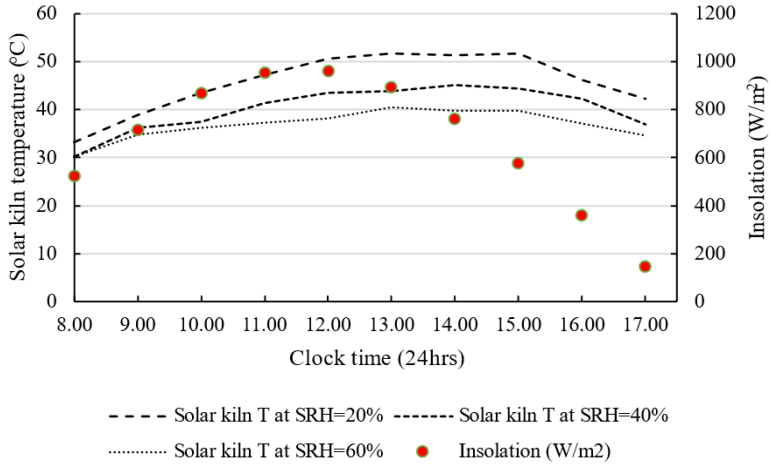

Figure 4. Comparison of the average insolation during the experiments and recorded temperatures in the solar kiln

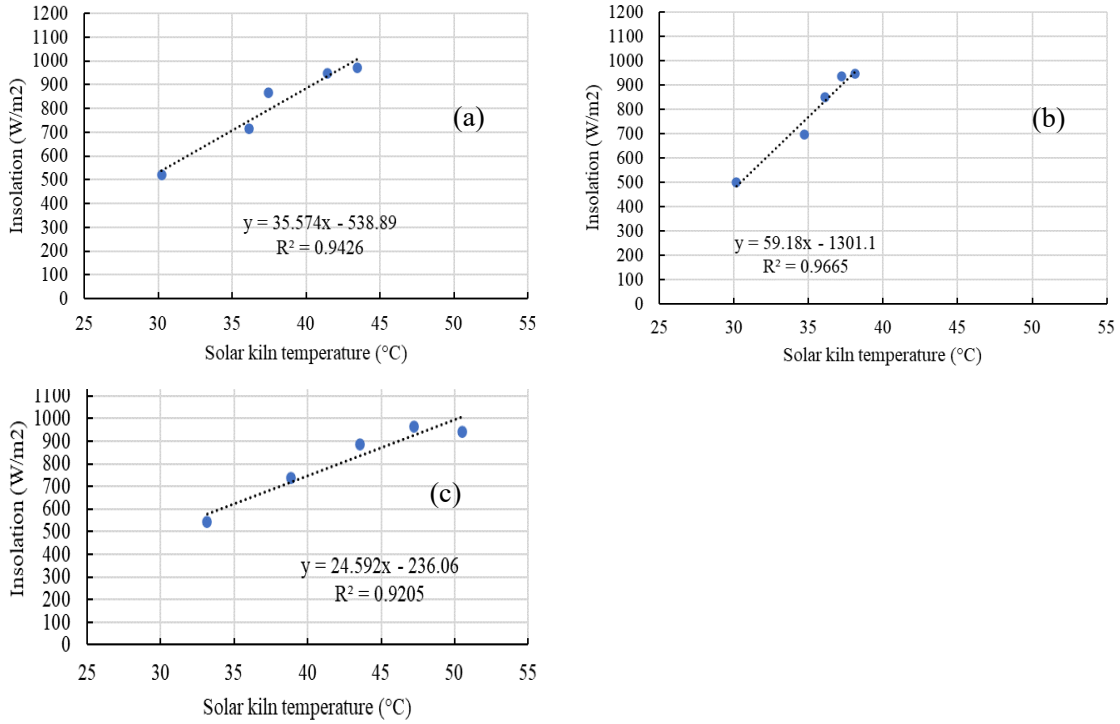

Figure 5. Solar kiln temperature as a function of available insolation at SRH of 20% (a); 40% (b); and 60% (c)

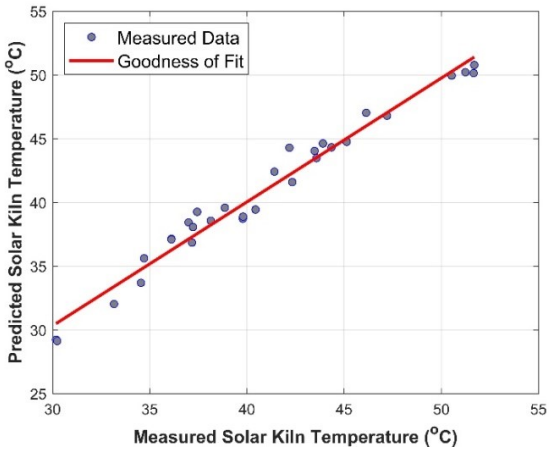

Figure 6: Plot of kiln temperature, predicted by equation (10), against measured temperature inside the experimental kiln

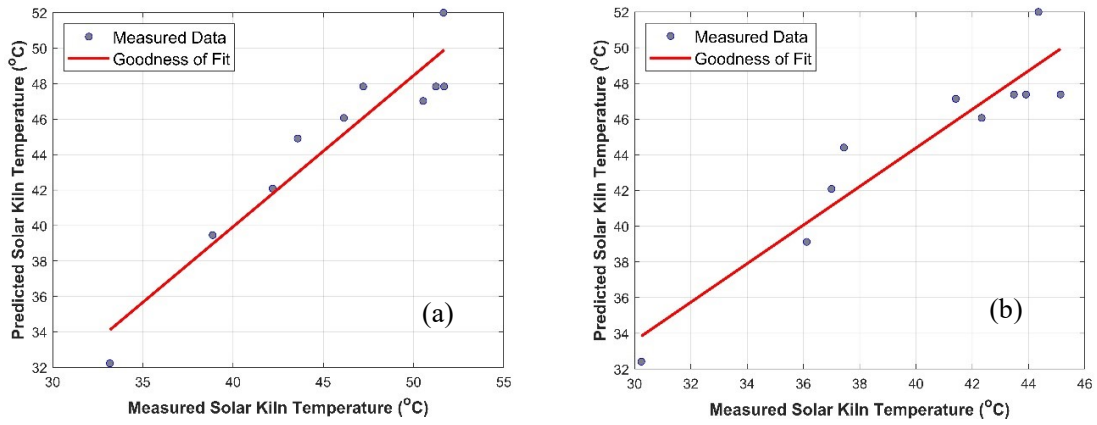

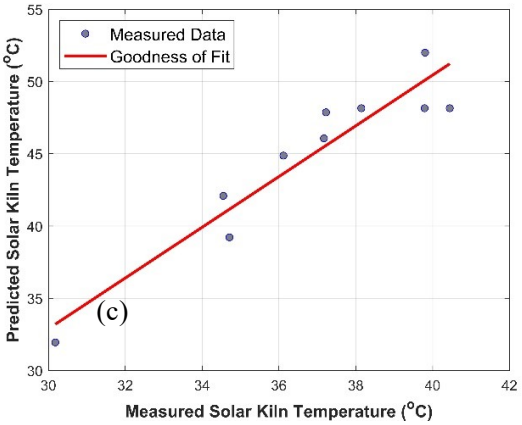

Figure 7. The relationship between the measured solar kiln temperature and the predicted solar kiln temperature; (a) RH=20%; (b) RH=40%; and (c) RH=60%

Table 1. Design of experiments on solar kiln performance

Experiments	Temperature (°C)	Relative humidity (%)	Clock time	Length of experiment (days)
1	60	20	08:00-17:00	10
2	60	40	08:00-17:00	10
3	60	60	08:00-17:00	10